Role of Groundwater Flow in Tile Drain Discharge

Peter J. Vaughan,* Donald L. Suarez, Jirka Simunek, Dennis L. Corwin, and James D. Rhoades

ABSTRACT

Tile systems drain water applied to agricultural fields as irrigation and precipitation but also may intercept regional groundwater flow. Identification and characterization of the potential sources of tile water is essential for informed management of salinity and contaminants. Factors influencing tile discharge including depth of water applied, evapotranspiration, water storage, drain blockage, and interception of regional groundwater flow were evaluated to determine which may be related to a fivefold variation in cumulative tile discharge among six sumps located 100 km west of Fresno, CA. Cumulative depths drained were calculated for 5 yr of weekly irrigation, precipitation, and discharge data. Evapotranspiration and water storage were estimated using the UnsatchemGeo variably-saturated water flow model. Well water levels measured on 19 dates were spatially-averaged providing spatial variation of depth-to-water among the drained areas. Variability in depth of water drained (0.18–0.95 m) was large and was not correlated with either water applied (3.26–4.58 m, $r^2 = 0.03$) or with computed water flux from the bottom of the soil column (0.05–0.31 m, $r^2 = 0.00$). Groundwater interception by tile drains was a factor because depth-to-water was negatively correlated with discharge ($r^2 = 0.42$) and drawdown of groundwater levels by drains was relatively larger for those drained areas encountered first during regional groundwater flow. For all six sumps, drained water is likely derived from locally applied water and interception of regional groundwater flow implying that standard two-dimensional models of flow to drains, representing only water applied locally, would not be applicable to modeling of drain flows or drain-water solute concentrations.

TILE DRAINAGE in agricultural areas provides a method of regulating the depth of shallow water tables. The water drained from tile systems is frequently not reusable as irrigation water because of high salinity and contamination. Two contaminants often present in the San Joaquin Valley of California are B and Se. Disposal of tile water in this area is a necessary component of a management system that includes tile drainage. But tile water disposal raises environmental concerns such as the well-known experience of Se contamination at Kesterson reservoir in the San Joaquin Valley. The source of tile water is shallow groundwater which may be derived from water applied during irrigation of a field, from local precipitation, or it may have moved laterally to the tile drain by regional groundwater flow. The determination of the relative importance of these components is significant because drainage of irrigation water represents an economic loss. Drainage of groundwater which has moved laterally from other areas is, however, not locally controllable and cannot be factored into the local economics of production. Regulation of drain water quality is therefore a complex issue because there are, potentially both local and regional components controlling water quality.

Tile drain tubes are normally installed in parallel sets with a fixed spacing. This arrangement can be modeled by analytical techniques which lead to expressions for flow rates within tubes based on drain diameter, spacing

and various boundary conditions for water flux and hydraulic head (Kirkham, 1949, 1958; Jury, 1975a; Fipps and Skaggs, 1991). The lower boundary condition of these models is an impervious layer which permits a solution using the method of images. This assumed boundary implies that all water arriving at a drain originated at the soil surface between the drains. In the analytical solutions, certain flow paths pass through lower elevations than the elevation of the drain resulting in upwards flow to the drains. Such paths may have travel times on the order of 10 yr or more (Jury, 1975b). The utility of the impervious layer assumption is questionable under certain field conditions as, for example, in the western San Joaquin Valley. In this area, a highly permeable sand layer underlies clay-rich soils that have much lower permeability (Deverel and Gallanthine, 1989; Belitz and Phillips, 1995). Groundwater flow is from southwest to northeast and the historic record of artesian wells at the margin of the alluvial fan near the San Joaquin River (Mendenhall et al., 1916) suggested that this groundwater flow was occurring in conditions where the groundwater level was close to the surface. Groundwater levels in this area were lowered by pumping during the first half of the 20th century, but the introduction of irrigation water from northern California, through the Delta-Mendota canal, and the installation of tile drainage have again stabilized the water table at a depth of 1.5 to 3 m (Deverel and Gallanthine, 1989). Water flowing to tile drains in this area is a mixture of local irrigation water and water that has moved upwards from the sand layer (Deverel and Fujii, 1988). Evidence for this partitioning includes isotopic enrichment of $\delta^{18}O$ with depth, and decreases in tritium concentrations when compared with irrigation water sampled at the same site (Deverel and Fio, 1991). Based on water chemistry data, the proportion of drained water that arrived from greater depths was 30% for a drain at 1.8-m depth and 60% for a 2.7-m drain. Furthermore, Se concentrations indicated that the deep groundwater component had arrived from the west (Deverel and Fio, 1991).

These geochemical studies of groundwater and tile-drained water on the west side of the San Joaquin Valley indicated that a significant portion of the water appearing in tile drains was not applied to the same field, but was water that had flowed upwards from greater depths and horizontally from the west.

In this study, we examined the water budget of an irrigated agricultural area located in the same general area of the western San Joaquin Valley as the aforementioned groundwater geochemical studies (Deverel and Gallanthine, 1989; Deverel and Fio, 1991). Considering

$$w_{et} + w_{ro} + w_{dp} + \Delta w_{st} + w_{td} - w_{ip} - w_{ig} = 0 \quad [1]$$

a water balance in terms of water depth [L] for a control volume consisting of a soil column and a tile drain. Water enters the volume as irrigation, precipitation or tile interception of groundwater and leaves as evapotranspiration, runoff, deep percolation, and tile drainage. The terms are: w_{ip} depth of water applied through irrigation and precipitation, w_{et} evapotranspiration, w_{ro} runoff, w_{dp} deep percolation, w_{td} tile drainage, Δw_{st} change in soil water storage (expressed as a depth of water within a soil column of specified height), and w_{ig} groundwater interception by tile drains. Spatial variability in the depth of water drained by tile systems could be caused by spatial variability in any of the amounts represented in Eq. [1] or by some combination these terms. The question addressed here was the origin of variability in depth of water drained given these spatially-variable processes.

MATERIALS AND METHODS

Field Area

The Broadview Water District is located on the west side of the San Joaquin Valley of California approximately 100 km west of Fresno. Most of the water district is divided into quarter-sections which are square fields with area of 64.8 ha. On the borders of the water district there are also some smaller fields with irregular shapes. This study was concerned with only quarter-sections, and henceforth we will refer to quarter-sections as fields. The district maintains irrigation turnouts in the southwest corner of each field. Water supplied from these turnouts is metered with a precision of 123 m^3 (0.1 acre-feet). Sumps are located in the northeast corner of certain fields for collection and disposal of water from tile-drain systems. Water draining into the sumps is pumped into drainage ditches and metered to the same precision as the irrigation water. The sumps may drain a single field, two adjacent fields, or all four fields that make up an entire section (Fig. 1). Because sumps may drain more than one field, the term *drainage area* is used to refer to the entire area drained by a sump.

Approximately 80% of the water district has tile drainage at approximately 1.8-m depth. The most common spacing of drain laterals is 91.4 m, but several other spacings are also present (Fig. 1). Maps of drains were compiled by the water district staff using data obtained from individual landowners. Six sumps were selected for analysis of irrigation and drainage, each located in the northeast corner of an entire section.

Every 2 d, cumulative flow meters for irrigation were read and weekly readings of meters on sumps were taken during the period of 1 Jan. 1991 to 1 May 1996 (the study period). Daily precipitation data, collected at the California Irrigation Management Information System (CIMIS) station 10 km east
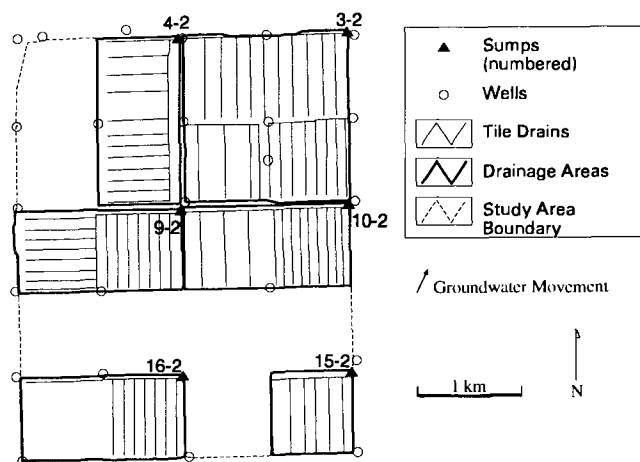

Fig. 1. Map of six drainage areas that drain to the numbered sump in the northeast corner of each area. Groundwater movement direction was a mean value computed for the entire water district using water table elevation data for 1991. Well locations are 24 of the 57 wells used in water table surface calculations.

of the study area, in Firebaugh, were combined with the irrigation data to generate a complete record of water applied to each field. There were probably minor differences in precipitation at the two locations but these differences were not significant for the analysis of spatial variability within the water district. For the summer growing seasons between 1991 and 1995, the land-use distribution for crops in the drainage areas was: 47% cotton (*Gossypium hirsutum* L.), 15% tomato (*Lycopersicon lycopersicum* L.), 11% alfalfa (*Medicago sativa* L.), 9% melon (*Cucumis melo* L.), and 18% fallow. No winter crops were grown during this period.

Simulation of Drainage from the Root Zone

Some terms in Eq. [1] can be evaluated easily from available data but others must be estimated. Evapotranspiration was an important component of the water balance but direct measurements of soil evaporation and transpiration were not available, so model calculation of evapotranspiration was necessary. In the San Joaquin Valley, crops such as cotton and alfalfa are often grown under conditions of periodic water stress, as a management tool, to increase crop production. A significant effect of water stress is reduction of transpiration from that of a fully-watered crop implying that daily transpiration can be considered as coupled to the soil water content. One model that includes coupling between these processes is the UnsatchemGeo model which computes variably-saturated water flow, plant root water uptake, multicomponent solute transport, and other processes occurring in the vadose zone (Vaughan et al., 1997). UnsatchemGeo is a generalization of the original Unsatchem model and operates in the context of a geographic information system (GIS), which stores both the data required by the model and the results. The original Unsatchem model is a finite-element solution of the Richards equation coupled to various numerical models of heat, multicomponent chemical, and carbon dioxide transport (Suarez and Simunek, 1994; Simunek and Suarez, 1994; Simunek et al., 1996; Suarez and Simunek, 1997). UnsatchemGeo models one-dimensional water flow and other processes at point locations within a geographic area. Data required by this model, such as initial water content as a function of depth, are specified for point locations. Other data, such as material properties, are specified for areas rather than points. The hierarchical nature of data organization in the model allows storage of data for points or areas and avoids unnecessary duplication of data. For the calculations described in this paper, the UnsatchemGeo model was set up to compute only water flow, plant root water uptake, heat flow, and root growth. The computed water flux at the lower boundary of the modeled soil column was of primary importance in this paper because it can be compared with the measured drainage.

Other terms in Eq. [1] that can be studied using UnsatchemGeo are the change in water storage (Δw_{st}) and runoff (w_{ro}). The surface boundary condition for water flow for the modeling described here was time-dependent, prescribed flux. At certain times, this prescribed flux exceeded the computed infiltration rate, resulting in ponding at the soil surface and an automatic reset to a constant head condition. Runoff was assumed for ponding depths >0.05 m. For a one-dimensional model this means ponding depths were limited to 0.05 m, and any further water application was considered runoff and was ignored. No measurements comparing runoff with surface water depth were available for the study area, so the ponding depth limitation of 0.05 m was simply a reasonable assumption.

At the lower boundary of the modeled soil column the specified flux boundary condition was the "deep drainage" condition (Simunek et al., 1996; Hopmans and Stricker, 1989),

$$q = -A \exp(-B|h - h_0|) \qquad [2]$$

where q is the flux [L^3 L^{-2} T^{-1}], A [L^3 L^{-2} T^{-1}], and B [L^{-1}] are parameters, and h_0 is the pressure head at the bottom node when the entire soil profile is fully-saturated [L]. For the calculations discussed here, A = 0.169 cm d^{-1} and B = 0.027 cm^{-1}.

Hydraulic properties required by the model were measured or estimated for the two main soil types that occur in the drainage areas. The soil types are the Lillis series (very fine, montmorillonitic, thermic Entic Chromoxererts) and the Cerini series (fine-loamy, mixed (calcareous), thermic Typic Torrifluvents) mapped by the Natural Resources Conservation Service (a preliminary, unpublished map based on soil surveys taken during 1990–1992). The measured hydraulic property was saturated hydraulic conductivity which was a mean value for two samples collected for each soil texture (Table 1). The two cylindrical soil samples (5.40 cm diam.) were collected using a bulk density sampler from a depth of 0.3 m at a spacing of 0.1 m. In 1991, a soil sampling operation collected soil samples from 315 locations within the Broadview Water District. From this sampling, an average saturation percentage for each soil type was determined by taking the mean for all samples collected from locations within the mapped area of that soil type. Locations for the soil sampling reported here, were selected from the sets of locations in the 1991 survey, as those which most closely matched the mean saturation percentage.

UnsatchemGeo uses the van Genuchten-Mualem model of water retention with $m = 1 - 1/n$,

$$\theta(h) = \begin{cases} \theta_r + \dfrac{\theta_s - \theta_r}{(1 + |\alpha h|^n)^{(1-1/n)}} & h < h_s \\ \theta_s & h \geq h_s \end{cases} \qquad [3]$$

where θ_s and θ_r are the saturated and residual water contents (cm^3 cm^{-3}), α (cm^{-1}) and n are empirical parameters, h (cm) is the pressure head, and h_s (cm) is the pressure head at saturation (van Genuchten, 1980; Simunek et al., 1996). θ_s, θ_r, α, and n were selected from a list of properties for a variety of soils (Carsel and Parrish, 1988). Error estimates for hydraulic properties given in Table 1 were not available because the values were either assumed, or, in the case of hydraulic conductivity, only two measurements were available.

Soil evaporation and plant transpiration were modeled through a combined potential evapotranspiration. Daily reference evapotranspiration, ET_0 (mm d^{-1}) was obtained from stored records representing conditions measured at the CIMIS station in Firebaugh. ET_0 in these records was calculated using the Penman equation (Penman, 1963). A potential crop evapotranspiration, T_p (cm d^{-1}) was obtained from

$$T_p = 0.1 \ ET_0 K_c \qquad [4]$$

where K_c is the crop coefficient (Doorenbos and Pruitt, 1977). The evapotranspiration was split into soil evaporation and

Table 1. Soil hydraulic properties.

Soil texture	Saturated water content	Residual water content	Parameters: [Eq. 3]		Saturated hydraulic conductivity†
			α	n	K_s (m/d)
	θ_s (cm^3 cm^{-3})	θ_r (cm^3 cm^{-3})	α (m^{-1})		
Sandy clay‡	0.45	0.10	2.7	1.23	0.016
Clay loam§	0.41	0.09	1.9	1.31	0.111

† Mean of measured values for two samples.
‡ Lillis series.
§ Cerini series.

plant transpiration under the assumption that the fractional rooting depth also represents the fraction of the evapotranspiration that is transpiration (Simunek et al., 1996). When the actual rooting depth reaches the maximum specified value, the canopy coverage of the soil is complete, the soil evaporation is zero, and the potential transpiration is equal to the potential evapotranspiration. Root water uptake at depth z was calculated using

$$T_c(z) = \alpha(h)\beta(z)T_p \qquad [5]$$

where $T_c(z)$ is the rate of water removal (cm cm^{-1} d^{-1}) with $\beta(z)$ the normalized root distribution function (cm^{-1}). The water stress function is

$$\alpha(h) = \frac{1}{1 + (h/h_{50})^p} \qquad [6]$$

where h_{50} is the pressure head causing a 50% reduction when the exponent $p = 1$ (see Simunek et al., 1996, for further details on root water uptake). The parameter h_{50} was set to -20 m and $p = 3$ in the calculations discussed here.

The UnsatchemGeo simulation of water flow in the various drainage areas was set to run over the study period. The initial condition for this simulation was volumetric soil water content, $\theta(z)$. The gravimetric soil water content was determined for samples collected at 0.3-m intervals to a depth of 1.2 m for each location (Lesch et al., 1992). A separate set of 75 measurements of bulk density taken both within the study area (Fig. 1), and in fields nearby, were kriged to obtain estimates of bulk density at sampling locations (Vaughan et al., 1996). $\theta(z)$ was computed using these estimates and was linearly interpolated between the sampling depths. The finite-element column extended to a maximum depth of 1.84 m. The time step was varied during the simulation depending on how rapidly convergence occurred during iteration of the water flow calculation. The minimum time step was 8.6 s and the maximum was 1 d. All changes in prescribed water flux at the soil surface were preceded by a gradual reduction of the time step to the minimum value.

Calculations were performed for two locations within each field. Cumulative drainage from the bottom of the modeled profile was compared with measured depths of drainage which were recorded on a weekly basis. Computed results were stored at time intervals varying from one to two days rather than at the computational time step to minimize data storage requirements. A subset of computed results was selected to match the dates when measurements were taken. Mean cumulative drainage depths for each drainage area were calculated as a simple arithmetic mean of the coincident data from all locations within the area.

Determination of Depth-to-Water

Groundwater levels throughout the study area were calculated from depth-to-water measured at 57 wells for 19 dates during the study period. These levels provided an independent data set for use in evaluating the role of groundwater in tile drainage. Because of equipment failures, the actual number of measured wells for any given date varied between 34 and 54 with a mean value of 48. The surface elevation of well sites was determined from a digital elevation model produced by the TOPOGRID[1] program (a modified version of an algorithm described by Hutchinson, 1989). Input data for the calculation

was a digital line graph file of topographic contour locations obtained from the U.S. Geological Survey. Elevation of the water table was determined, for each well, by subtracting the the measured depth-to-water from the computed surface elevation. The resulting water table elevations were fitted using a third-order trend surface. Residuals for water table elevations were calculated at each well location. These residuals were kriged to provide an improved representation of each surface

$$z_{est} = z_t + z_k \qquad [7]$$

(z_{est}) where z_t is estimated from the trend surface and z_k is estimated by kriging the residuals. Kriging permitted better representation of the variability at shorter distances. All kriging calculations used the ordinary kriging program (OKB2D) in the GSLIB package (Deutsch and Journel, 1992). For the water table elevations and residuals, the surfaces were represented as grids with cell size of 20 m. Spatial covariance was modeled for semivariogram data for each of the 19 dates. These models normally included a small nugget effect (mean of nugget values: 0.016 m^2) and an omnidirectional spherical model but the residuals for 2 of the 19 dates required directional modeling.

RESULTS AND DISCUSSION

During the 1948 d represented in the study period, cumulative tile drainage for the six fields was a maximum depth of 0.95 m in field 16-2 and a minimum of 0.18 m in field 9-2, a factor of five variation (Fig. 2). This variation in depth drained was also consistent over time. The main question, addressed here, was the origin of this variability in depth of water drained. Some possible contributing factors were: different amounts of irrigation water applied to the fields, different degrees of water use caused by planting different crops, spatial variability of Δw_{st} [Eq. 1], blockage of tile drains causing reduced flow and correspondingly greater deep percolation to the groundwater, lateral groundwater flow to the sump drainage area, and variation of hydraulic conductivity for different soil types causing variability in the efficiency of the drains.

Variation in cumulative depth of applied water among the drainage areas was 3.26 to 4.58 m depth, or a factor of 1.4. This was significantly less than the factor of five
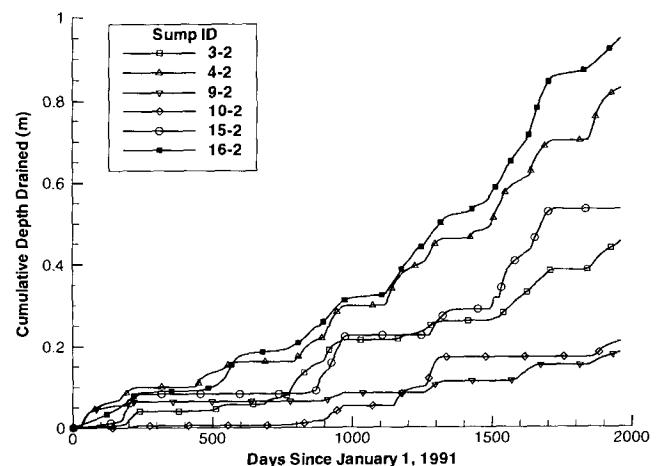

Fig. 2. Cumulative depth of water drained from six drainage areas by tile drain systems between 1 Jan. 1991 and 1 May 1996.

---

[1] A program in the ARC/INFO software package. The use of brand names in this report is for identification purposes only and does not constitute endorsement by the USDA.

variation that occurred for the cumulative drainage depths (Fig. 3). Furthermore, the depth of water applied and depth drained for specific fields were poorly correlated (coefficient of determination, $r^2 = 0.03$). The drainage area with the greatest drainage depth had the lowest depth of applied water (16-2). Also, the greatest depth of applied water (4.6 m) was almost identical for two drainage areas (3-2 and 4-2), but the depth drained for these areas differed by a factor of 1.8. The data for drainage area 4-2 did suggest a positive correlation because 4-2 had the greatest depth of applied water and the second largest cumulative drainage. But, considering the entire data set, there was only a small, poorly-correlated variation in irrigation amount, implying that variations in drainage depths are probably better explained by other factors.

Spatial variability in water storage is likely to be significant in the analysis of cumulative drainage for short modeling periods. But variations in water storage are restricted to a finite range of soil water content implying that such variations will be less significant as the modeled time period increases. Δw_{st} [Eq. 1] is expressed as the change in depth of water over the 1.84 m modeled soil column. For the 5-yr period, computed Δw_{st} varied from a mean value of -0.11 m in drainage area 4-2 to 0.10 m in 10-2. This variation was not negligible and suggested that spatial variation of soil water storage was a potential contributing factor to the observed variations in drainage. However, the variation was not large enough to consider spatial variation in Δw_{st} as a major factor in the 0.8 m variation in cumulative drainage depth.

Compared with irrigation and precipitation amounts, the explanation of drainage variability based on spatial variation of evapotranspiration rates was less certain because there was no source of continuous evapotranspiration estimates from measured data within individual fields. However, evapotranspiration was computed by the UnsatchemGeo program using the plant root water uptake module. The calculated cumulative drainage from the base of the modeled profile predicted the frac-

tion of applied water that was drained. The remaining fraction was either removed by evapotranspiration or was stored in the profile. Because this study attempted to determine whether variability in evapotranspiration could have resulted in the observed variability in drainage, a conservative assumption was that the entire computed flow entered the tile drains and appeared at the sump. This assumption was equivalent to $w_{dp} = 0$ [Eq. 1], and would tend to maximize the effect of variability in evapotranspiration. The difference between observed and modeled drainage, termed the drainage residual in this paper, was plotted to demonstrate the degree to which variability in observed drainage can be explained by the model (Fig. 4). The model made substantially better predictions of observed drainage for sumps 3-2, 9-2, and 10-2 than for sumps 4-2, 15-2, and 16-2. Predicted and observed cumulative drainage for each set of sumps, taken separately, were positively correlated. But, when the data were combined, the correlation became nonexistent ($r^2 = 0.00$). By subtracting an arbitrary 0.5-m depth from the measured depths for sumps 4-2, 15-2, and 16-2, the correlation for all six sumps was improved ($r^2 = 0.45$). This suggested that poor model performance, indicated by the nonexistent correlation, could have been caused by additional water, from some other source, that entered sumps 4-2, 15-2, and 16-2. In summary, while variations in evapotranspiration among different fields might have been a secondary contributing factor to observed variability in cumulative drainage, such variations were not a prime factor.

Variations in cumulative drainage depths could also be caused by drain blockage. Although such variations were not directly quantifiable because no data were available regarding performance of individual drain laterals, some observations of relative drainage rates were relevant. The least cumulative depths drained occurred for sumps 9-2 and 10-2 whereas the greatest depths drained occurred at sumps 4-2 and 16-2. If blockage were an important factor, then the argument would be that drains in 9-2 and 10-2 tended to have more blockage, resulting in slower flow rates. Drainage areas
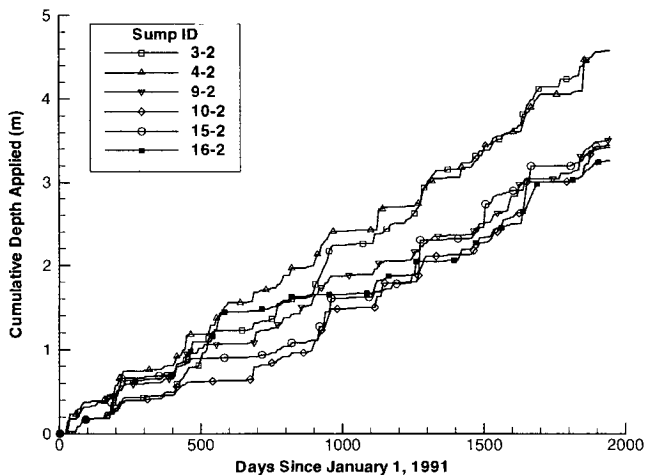

Fig. 3. Cumulative depth of water (irrigation + precipitation) applied to six drainage areas designated by the sump identification number between 1 Jan. 1991 and 1 May 1996.
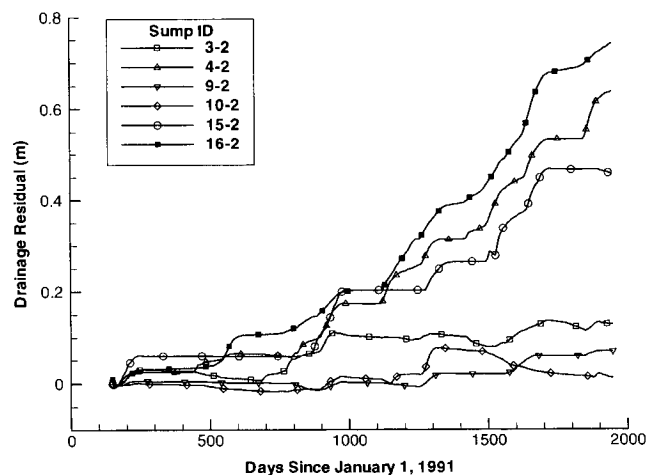

Fig. 4. Cumulative drainage depth residual (observed − calculated). Drainage depths were calculated assuming all water drained from the soil column entered the tile drains.

9-2 and 10-2, however, have the greatest density of tile drains and the slowest drainage rates (Fig. 5). It seemed unlikely that tile drain blockage would have been more significant in fields where the density of drains was greatest. Also, there was no specific evidence of substantial tile drain blockage in drainage areas 9-2 and 10-2 (David Cone, manager of the water district, 1998, personal communication). Finally, drainage area 16-2 only had a main drain running east-west at the northern end of the western field (Fig. 1), there are no tile drain laterals. This accounted for the low tile drain density in this drainage area. The lack of tile drain laterals could be thought of as a hypothetical blockage of all drains in this field except the main drain. Drainage area 16-2 had the highest cumulative depth drained, however, so the complete elimination of flow from the hypothetical set of drain laterals in half of the drainage area resulted in no reduction of cumulative drainage depths relative to other areas. This was quite surprising, but it certainly suggested that blockage of tile drain laterals was unlikely to have been an important factor in this drainage area. A more reasonable conclusion is that, over long time periods, flow within tile drains in the study area was probably not the rate-controlling factor for sump drainage rates.

The fifth possibility, groundwater flow into drains, was difficult to evaluate because the flux of groundwater into the drains cannot be calculated accurately. Instead, the approach we chose was calculation of mean depth-to-groundwater within drainage areas, and comparison of these depths with mean daily drainage. If depth-to-groundwater were a significant factor then there should have been a negative correlation between depth-to-groundwater and mean daily drainage at least for groundwater depths that were shallower than the depth of the drains. Modeling of water table elevation was done to obtain estimates of the mean depth-to-water within each drainage area for each of the 19 sets of measurements of depth-to-water. The addition of the kriged residual surface to the original third-order trend surface substantially improved the fit [Eq. 7]. The tem-

porally-averaged sum of squares taken over the 19 dates was 6.22 m^2 for the trend surface, but only 0.80 m^2 when the kriged surface was added. The kriged surface was not an exact interpolation because of the non-zero nugget effect.

Comparison of well levels and mean daily depth drained was done for the period between 1 Jan. 1991 and 2 Jan. 1996 (Fig. 6). This final date was the date of the last well-level measurement during the study period. The estimated mean depth-to-water, z_{est} [Eq. 7], was spatially averaged over each drainage area by taking the arithmetic mean for all grid cells located within the area including an areal weighting to accommodate those cells along the boundaries which are smaller than 20 by 20 m. This was done for each measurement date. These results were temporally-averaged over the 19 dates to obtain a mean depth-to-water. Resulting mean depths were likely biased from the true mean depth-to-water because the dates of the measurements did not follow a sampling strategy that would adequately characterize the seasonal fluctuations in water levels. Nonetheless, if there was spatial variation in depth-to-water that was negatively correlated with daily depth drained, such spatial variation should have been apparent even if the computed means did not represent true mean values because the seasonal fluctuations were approximately the same at all sites. The results were consistent with negative correlation of mean daily depth drained and mean depth-to-water (coefficient of determination, $r^2 = 0.42$, Fig. 6). A regression model, such as a linear model, was not plotted because the functional form of the relationship is likely to exhibit a threshold depth-to-water occurring whenever the depth-to-water is less than the depth of the bottom of the drain. A rapid increase in drain flows would be expected as the mean water table moves upwards above the drains. The data were generally consistent with a threshold model of drain flow because the three greatest depths drained occurred in drainage areas having the three smallest values of depth-to-water. However, there are not enough data to adequately characterize a threshold
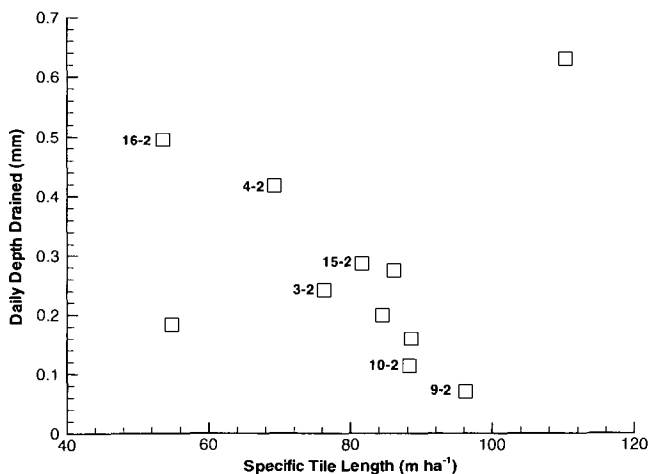

Fig. 5. Mean daily depth of water drained vs. areal density of drains for several drainage areas. Non-numbered points represent drainage areas that surrounded the study area.
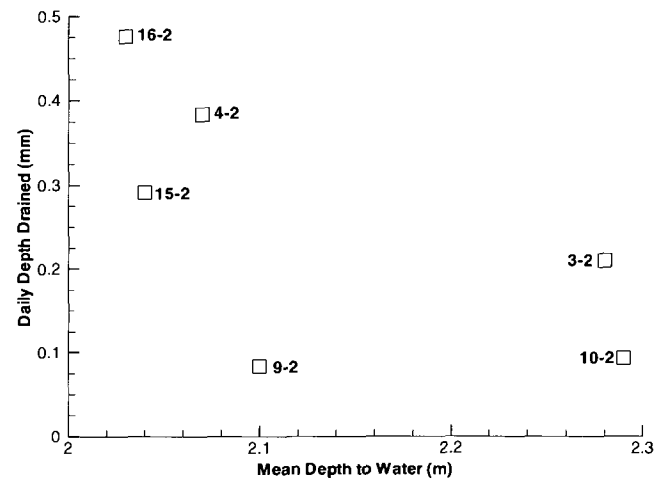

Fig. 6. Mean daily depth drained was spatially-averaged within each drainage area and temporally-averaged for the 19 dates when measurements were made.

model, and the mean depth-to-water was likely biased by the sampling such that it could not be compared to the actual depth of the drains.

Other evidence, based on groundwater movement, also supported the idea that regional groundwater was flowing into tile drains. The groundwater movement direction (north-northeast) was calculated from the average slope of the water table surface in 1991 (Fig. 1). Water levels in six wells located along an east-west road, 0.8 km south of the study area, were compared with data from all other wells in the district (Fig. 7). The mean well depths for these six wells were slightly greater than mean well depths for the remaining wells in the district during 1991 but, starting in late 1992, these well depths were consistently less than those in the remainder of the district. This trend continued through June of 1997, as indicated by the last point on the plot. Thus, for most of the study period, depth-to-water was actually less at locations upslope from the drainage areas. Two of the three drainage areas showing the greatest cumulative depth drained were located near the southern boundary of the water district (15-2 and 16-2). Groundwater moving north-northeast from areas to the south and west of the district would encounter these tile drain systems first and the maintenance of groundwater levels at tile drain depths would tend to require higher flows of nonlocal groundwater in these sumps. The two drainage areas with the lowest cumulative drainage amounts (9-2 and 10-2) were not in the direct path of groundwater moving into the district from the south and would be expected to drain less groundwater, as observed (Fig. 2). Thus, drainage in areas 9-2, 10-2, 15-2, and 16-2 can be rationalized by this argument based on groundwater movement. Mean depth-to-water in drainage area 4-2 was 2.0 m, essentially the same as the mean depth-to-water in 15-2 and 16-2. Area 4-2, however, was located in the interior of the water district so the high groundwater level and large cumulative depth drained would not be explained by groundwater movement. The depth of water applied in 4-2 was equal to that applied to 3-2

and approximately 1.2 m more than the depth applied to the other drainage areas during the 5-yr period. Depth of water applied was, therefore, probably a factor in the greater amount of drainage in this drainage area. Cumulative depth drained in drainage area 3-2 was somewhat greater than for 9-2 and 10-2, but the simulation of depth drained for 3-2 brought the drainage residual close to those of 9-2 and 10-2 (Fig. 4). Thus, spatial variation in evapotranspiration and/or hydraulic conductivity could account for the variation in depth drained among 3-2, 9-2, and 10-2.

Because regional groundwater flow to tile drains was not easily quantifiable, another approach involved examining relationships between the factors that were likely related to groundwater movement and the observed drainage. One such factor was saturated hydraulic conductivity which varied by a factor of 7 for the two soil textures present in the study area (Table 1). Greater saturated hydraulic conductivities would be expected to result in more rapid drainage of irrigation water or groundwater. For irrigation water, greater hydraulic conductivities would be expected to drain water more rapidly out of the root zone to the groundwater level, reducing evapotranspiration losses. More rapid drainage of groundwater that has moved laterally would be expected for the clay-loam soil which occurs in north-northeast-trending stringers. Thus, variations in areal fraction of clay-loam among the fields might have been related to the effectiveness of removal of either type of water by tile drains. The areal fraction of clay-loam, in each drainage area, was determined using a GIS overlay procedure. The data set was expanded to include some other drainage areas for which modeling data were not available. The data for daily depth drained versus areal fraction of clay-loam were not correlated based on the available data (coefficient of determination, $r^2 = 0.002$, Fig. 8). Thus, a straightforward conclusion that greater drainage rates occurred in areas that had a greater areal fraction of clay-loam was not supported by these data.

Fig. 7. Depth-to-water is an arithmetic mean for well depths that were measured on each specific date. Triangles represent six wells along the southern boundary of the water district. Squares represent all the remaining wells.

Fig. 8. Areal percent of each soil texture was determined for each drainage area from GIS overlays of a preliminary soil texture map based on a 1990 to 1992 soil survey of the area by the Natural Resources Conservation Service.

CONCLUSIONS

In this 5-yr study of Broadview Water District irrigation and drainage records we have shown that variability in cumulative tile drain flows could not be uniquely explained by specific local variations in any one of the following factors: irrigation amount, evapotranspiration, variation in water storage, or tile drain blockage. Drainage depths that were consistently higher for certain sumps were especially difficult to rationalize on the basis of yearly irrigation amounts which were quite consistent among the various fields. All these factors, however, may have possibly contributed to the observed variability and there were probably interactions among them. Another possible explanation was variation in the fraction of nonlocal groundwater appearing at different sumps. Evidence for this was negative correlation of groundwater levels and cumulative depth drained. In addition, greater cumulative depths of drainage occurred in the two drainage areas that would be encountered first by groundwater moving in a north-northeast direction. The relatively large depth drained by one sump near the northern boundary of the water district was probably not related to lateral groundwater flow but might be explained by the greater amount of irrigation water applied to that drainage area. Because several of the possible explanations that were presented might be operable to different degrees and might exhibit interactions, it was not possible to complete a quantitative evaluation of the fractional contribution by each process. In general, caution is warranted when modeling tile-drain flow or the chemical composition of tile drain waters because mixing with groundwater that was transported laterally from other areas may be occurring. Furthermore, this study, and the earlier work cited (Deverel and Gallanthine, 1989; Deverel and Fio, 1991), suggest that any modeling of tile drain flows in this area which requires the assumption of a shallow impermeable layer and no mixing of drained irrigation water with non-local groundwater will have poor predictive capability unless it can be independently confirmed that such mixing is not occurring.

ACKNOWLEDGMENTS

REFERENCES

Belitz, K., and S.P. Phillips. 1995. Alternative to agricultural drains in California's San Joaquin Valley: Results of a regional-scale hydrogeologic approach. Water Resour. Res. 31:1845–1862.

Carsel, R.F., and R.S. Parrish. 1988. Developing joint probability distributions of soil water retention characteristics. Water Resour. Res. 24:755–769.

Deutsch, C.V., and A.G. Journel. 1992. GSLIB geostatistical software library and user's guide. Oxford Univ. Press, New York.

Deverel, S.J., and J.L. Fio. 1991. Groundwater flow and solute movement to drain laterals, western San Joaquin Valley, California 1. Geochemical Assessment. Water Resour. Res. 27:2233–2246.

Deverel, S.J., and R. Fujii. 1988. Processes affecting the distribution of selenium in shallow groundwater of agricultural areas, western San Joaquin Valley, California. Water Resour. Res. 24:516–524.

Deverel, S.J., and S.K. Gallanthine. 1989. Relation of salinity and selenium in shallow groundwater to hydrologic and geochemical processes, western San Joaquin Valley, California. J. Hydrol. 109:125–149.

Doorenbos, J., and W.O. Pruitt. 1977. Guidelines for predicting crop water requirements. Irrigation and Drainage Paper 24. FAO, Rome.

Fipps, G., and R.W. Skaggs. 1991. Simple methods for predicting flow to drains. J. Irrig. Drain. Eng. 117:881–896.

Hopmans, J.W., and J.N.M. Stricker. 1989. Stochastic analysis of soil water regime in a watershed. J. Hydrol. 105:57–84.

Hutchinson, M.F. 1989. A new procedure for gridding elevation and stream line data with automatic removal of spurious pits. J. Hydrol. 106:211–232.

Jury, W.A. 1975a. Solute travel-time estimates for tile-drained fields: 1. Theory. Soil Sci. Soc. Am. J. 39:1020–1024.

Jury, W.A. 1975b. Solute travel-time estimates for tile-drained fields: II. Experimental. Soil Sci. Soc. Am. J. 39:1024–1028.

Kirkham, D. 1949. Flow of ponded water into drain tubes in soil overlying an impervious layer. Trans. Am. Geophys. Union. 30: 369–385.

Kirkham, D. 1958. Seepage of steady rainfall through soil into drains. Trans. Am. Geophys. Union. 39:892–908.

Lesch, S.M., J.D. Rhoades, and D.L. Corwin. 1992. Statistical modeling and prediction methodologies for large scale spatial soil salinity characterization: A case study using calibrated electromagnetic measurements within the Broadview Water District. U.S. Salinity Lab. Tech. Rep. 131. U.S. Salinity Lab., Riverside, CA.

Mendenhall, W.C., R.B. Dole, and H. Stabler. 1916. Ground water in the San Joaquin Valley, California. U.S. Geol. Surv. Water Supply Paper 398. U.S. Gov. Print. Office, Washington, DC.

Penman, H.L. 1963. Vegetation and hydrology. Tech. Comm. 53. Commonwealth Bureau of Soils, Harpenden, England.

Simunek, J., and D.L. Suarez. 1994. Major ion chemistry model for variably saturated porous media. Water Resour. Res. 30:1115–1133.

Simunek, J., D.L. Suarez, and M. Sejna. 1996. The Unsatchem software package for simulating the one-dimensional variably saturated water flow, heat transport, carbon dioxide production and transport, and multicomponent solute transport with major ion equilibrium and kinetic chemistry. Version 2.0. U.S. Salinity Lab. Res. Rep. 141. U.S. Salinity Lab., Riverside, CA.

Suarez, D.L., and J. Simunek. 1994. Modeling equilibrium and kinetic major ion chemistry with CO_2 production/transport coupled to unsaturated water flow. p. 1215–1246. In G.W. Gee and N.R. Wing (ed.) In-situ remediation: Scientific basis for current and future technologies. Part 2. Thirty-third Hanford Symposium on Health and the Environment, Pasco, WA. 7–11 Nov. 1994. Batelle Press, Richland, WA.

Suarez, D.L., and J. Simunek. 1997. UNSATCHEM: Unsaturated water and solute transport model with equilibrium and kinetic chemistry. Soil Sci. Soc. Am. J. 61:1633–1646.

van Genuchten, M.Th. 1980. A closed-form equation for predicting the hydraulic conductivity of unsaturated soils. Soil Sci. Soc. Am. J. 44:892–898.

Vaughan, P.J., J. Simunek, D.L. Suarez, D.L. Corwin, and J.D. Rhoades. 1996. UnsatchemGeo: Modeling water flow and multicomponent solute transport in a GIS context. p. 235–246. In D.L. Corwin and K. Loague (ed.) Applications of GIS to the modeling of non-point source pollutants in the vadose zone. SSSA Spec. Publ. 48. SSSA, Madison, WI.

Vaughan, P.J., D.L. Suarez, J. Simunek, D.L. Corwin, and J.D. Rhoades. 1997. UnsatchemGeo geographic information system software package for simulating one-dimensional water flow, heat transport, carbon dioxide transport, and multicomponent solute transport in a geographic area. Version 1. U.S. Salinity Lab. Res. Rep. 142. U.S. Salinity Lab., Riverside, CA.